Published in final edited form as:

Food Addit Contam Part A Chem Anal Control Expo Risk Assess. 2020 February ; 37(2): 332–341. doi: 10.1080/19440049.2019.1662493.

A high capacity bentonite clay for the sorption of aflatoxins

Meichen Wang, **Sara E. Hearon**, **Timothy D Phillips***

Veterinary Integrative Biosciences, College of Veterinary Medicine and Biomedical Sciences, Texas A&M University, College Station, Texas 77845, United States

Abstract

Previously a calcium bentonite clay (CB) has been shown to tightly bind aflatoxins *in vitro*, significantly reduce mortality and morbidity in animals, and decrease molecular biomarkers of aflatoxin exposure in humans and animals. Extensive studies have shown that CB is safe for human and animal consumption. In further work, we have investigated a highly active sodium bentonite (SB) clay (SB-E) with enhanced aflatoxin sorption efficacy compared to CB and other clays. Computational models and isothermal analyses were used to characterize toxin/clay surface interactions, predict mechanisms of toxin sorption, and gain insight into: 1) surface capacities and affinities, and 2) thermodynamics and sites of toxin/surface interactions. We have also used a toxin-sensitive living organism (*Hydra vulgaris*) to confirm the safety and predict the efficacy of SB-E against aflatoxin toxicity. Compared to CB, SB-E had a higher capacity for aflatoxin B_1 (AfB_1) at pH 2 and 6.5. Results from this work suggest that high capacity clays such as SB-E can be used as effective aflatoxin enterosorbents to decrease short-term exposures in humans and animals when included in food and/or water during extended droughts and outbreaks of aflatoxicosis.

Keywords

Aflatoxin; bentonite; sorption; enterosorbent; mycotoxin; isotherms; hydra bioassay

Introduction

Aspergillus flavus and *Aspergillus parasiticus* are fungi that produce highly toxic and carcinogenic metabolites known as aflatoxins. The aflatoxins are widespread and can frequently cause health problems during extended periods of heat and drought. Every year a significant percentage of the world's grain and oilseed supply is contaminated with aflatoxins, and this contamination of the diet can result in disease and death, especially in vulnerable populations of humans and animals (CAST 1989; Phillips et al. 1995). Dairy animals can also secrete carcinogenic metabolites in their milk (aflatoxin M_1) following the ingestion of aflatoxin-contaminated feed, resulting in unintended aflatoxin exposures from milk and dairy products (Allcroft and Carnaghan 1963). Among the naturally occurring

*Correspondence: tphillips@cvm.tamu.edu.

Declaration of interest statement

The authors declare no conflict of interest.

aflatoxins, aflatoxin B_1 (AfB_1) is the most toxic and is commonly detected in diverse food and feed products (Grant and Phillips 1998). Common symptoms in humans and animals from AfB_1 exposure include growth stunting, weight loss, liver toxicity, immunosuppression and hepatocellular carcinoma (Murugesan et al. 2015; Wang et al. 2017).

Detection and quantification of aflatoxins in contaminated grains are difficult because of heterogeneous distribution of mold contamination. The majority of a feed may be below the action level of 20 ng g^{-1} (CAST 1989), but small portions can contain much higher levels (hot spots), which can affect the final concentration and toxicological outcome after processing and mixing. Because of the widespread occurrence of aflatoxins and the potent carcinogenicity of AfB_1, practical and effective detoxification methods are needed.

Innovative enterosorption strategies to significantly diminish the bioavailability of aflatoxins and reduce human and animal exposures from contaminated food and feed have been developed. Smectite clays (including bentonites) consist of three-layered molecular sheets containing two layers of silica that are tetrahedrally coordinated to oxygen and one layer of alumina that is octahedrally coordinated to oxygen. The sheets are weakly bonded which allow water and chemicals to enter. They have large surface areas, which result in swelling and considerable expansion when saturated and shrinkage when drying. These clays are sticky and plastic when wet and can pose problems with shear and consolidation (USDA 1978; EC 2005). Ca^{2+}/Na^{+}-bentonite with 20% (or more) sodium, behaves qualitatively as a sodium bentonite clay (SB), whereas bentonite with 90% (or more) calcium in the interlayer behaves similarly to calcium bentonite (CB) (Thuresson et al. 2017). Previously, our laboratory has conducted a series of *in vitro* studies, which have demonstrated that a CB can tightly bind AfB_1 with high capacity. Its global inclusion into feedstuffs and food has been reported to protect numerous animal species and to significantly reduce biomarkers of AfB_1 exposure in humans (Phillips et al. 2019). The mechanism of protection involves sorption of AfB_1 onto active interlayer surfaces of the bentonite, resulting in a reduced concentration of unbound toxin in the gastrointestinal tract and decreased bioavailability and toxicity of AfB_1. Results from our earlier work with bentonites have indicated that these clays possess active sites within their interlamellar regions for aflatoxin sorption. The carbonyl moiety in the aflatoxin molecule is important for binding. Thermodynamic studies have shown that the reaction is spontaneous in the forward direction and involves chemisorption of aflatoxins to bentonite with heats of sorption, or enthapies (ΔHs) equal to > -40 kJ/mol. Stereochemistry and planar surfaces of the aflatoxin ring (minus the terminal furan), favor the interaction and result in tight binding. Other reports have suggested that aflatoxin sorption mechanisms may include electron donor-acceptor, ion-dipole interactions, coordination between exchange cations and the carbonyl oxygens, and water bridging (Phillips et al. 2019).

A variety of aflatoxin mitigants including: natural binders, such as bentonite clay and chemopreventive agents such as green tea polyphenols (Tang et al. 2008), chlorophyllin (Egner et al. 2001), oltipraz (Wang et al. 1999) and sulforaphane (Kensler et al. 2005), have been tested in human studies. The bentonite clay, unlike the chemopreventive agents, can work rapidly to bind toxins in the stomach and intestines, thus decreasing bioavailability and toxicity. Due to high affinity, high capacity and a large heat of sorption for aflatoxin onto CB

surfaces, it can be used therapeutically to prevent mortality and decrease morbidity during acute outbreaks of aflatoxicosis in the vulnerable. Importantly, CB clay has been reported to be very cost-effective at $0.73 per person per year (Khlangwiset and Wu, 2010). Unlike CB, SB clay is known for its higher expansibility (swelling) in water, resulting in more prominent delamination, less selective sorption and similar, or less, binding capacity than that of the CB.

A wide range of materials used in aflatoxin sorption studies have shown limited adsorption capacities, low capacities, or no capacity for toxin binding based on isothermal data and curve fitting using Langmuir and Freundlich models. The purpose of this study was to investigate a sodium bentonite sample (SB-E) that was unique to other bentonite samples (sodium and calcium) based on a combination of expansibility, flocculation rate and aflatoxin adsorption. Computational models and isothermal analyses were used to delineate sorption mechanisms and to predict the thermodynamics of aflatoxin binding to active sites on the clays. Equilibrium isothermal analyses were conducted to derive binding parameters and to gain insight into: 1) surface capacities and affinities, and 2) thermodynamics of toxin/surface interactions. We have also used a toxin-sensitive living organism (*Hydra vulgaris*) to confirm the safety and predict the efficacy of these sorbents against AfB_1.

Materials and Methods

Reagent

AfB_1 was purchased from Sigma Aldrich (Saint Louis, MO). In this study, CB standard was obtained from BASF Chemical Company (Lampertheim, Germany) with an average total surface area as high as 850 $m^2\ g^{-1}$, an external surface area of approximately 70 $m^2\ g^{-1}$ and cation exchange capacity equal to 97 cmol kg^{-1} (Grant and Phillips 1998). SB standard was a gift from the Source Clay Mineral Repository at the University of Missouri-Columbia with an estimated cation exchange capacity equal to 75 cmol kg^{-1}. The generic formula for these clays is $(Na,Ca)_{0.3}(Al,Mg)_2Si_4O_{10}(OH)_2{\cdot}nH_2O$. Samples of both clays contain some quartz, mica, calcite, orthoclase feldspars and sanidine as impurities, and mesopores of approximately 5 nm diameter (Marroquin-Cardona et al. 2011). The novel SB sample (SB-E) listed as a hydrated sodium calcium aluminosilicate (HSCAS) from Halliburton (Houston, TX). Diverse important physico-chemical properties of CB, SB and SB-E have been summarized in Table 1. Ultrapure deionized water (18.2 MΩ) was generated in the laboratory using an Elga™ automated filtration system (Woodridge, IL) and was used in all experiments.

In order to confirm the importance of an intact interlayer and investigate potential aflatoxin binding sites, the interlayers of sample sorbents were collapsed by heating at 200°C for 30 min followed by 800°C for 1 hr (Wang et al. 2019).

Coefficient of Linear Expansibility in Water

Sorbent samples were added to the 2 mL mark in graduated cylinders, and then stirred with 20 mL of water. After 24 hr following hydration and swelling, the final sorbent volume was determined. The ratio that was calculated from the beginning (2 mL of clay) and the final

volume was indicative of hydration and expansion of the sample. A higher ratio indicates greater hydration and expansion.

In Vitro Isothermal Sorption

The AfB_1 stock solution was prepared by dissolving pure crystals of AfB_1 into acetonitrile. A calculated amount of the stock solution was injected into distilled water at pH 6.5 (the average pH of human intestine) or pH 2 (the average pH of human stomach) to yield an 8 mg kg^{-1} (8 μg/mL) AfB_1 solution that was used for each isothermal study (Fallingborg 1999). The concentration was confirmed by scanning and reading the absorbance of aflatoxin at 362 nm using the SHIMADZU UV-visible spectrophotometer (UV-1800, SHIMADZU Corporation, Japan). The maximum AfB_1 concentration was set at 8 mg kg^{-1} (well below the solubility range of 11–33 mg kg^{-1} for aflatoxins) so that precipitation of AfB_1 did not occur in the solutions. Then 100 μg of each sorbent was exposed to an increasing concentration gradient of AfB_1 solution: 0.4, 0.8, 1.6, 2.4, 3.2, 4, 4.8, 6, 6.4, 7.2 and 8 mg kg^{-1}. The concentration gradients were achieved by adding a calculated amount of aflatoxin solution along with a complementary volume of distilled water to sterile 17 × 100 mm polypropylene centrifuge tubes to make a total volume of 5 mL. The 100 μg sorbent inclusion was achieved by injecting 50 μL of a 2 mg mL^{-1} clay suspension into the reaction media. Besides testing samples, there were 3 controls consisting of 5 mL each of distilled water, 8 mg kg^{-1} AfB_1 solution without sorbent and 100 μg sorbent in distilled water. The control and test groups were capped and agitated at 1000 rpm for 2 hr at ambient temperature (26°C) and body temperature (37°C) using the IKA® electric shaker (VIBRAX VXR basic, Werke, Germany). All samples were then centrifuged at 2000 g for 20 min to separate the clay/AfB_1 complex from solution. The UV-visible spectrophotometer was used to measure the free AfB_1 in the supernatant from test and control groups.

Data Calculations and Curve Fitting

The UV-visible absorbance data were used to calculate the concentration of AfB_1 left in solution using Beer's law. The amount of toxin bound by clay at each data point was derived from the concentration difference between test and control groups and expressed as mol/kg on the isotherm. Values were calculated by the difference in moles of free toxin in the test solution versus control groups and is then divided by the mass of the clays included.

These data were then plotted using Table-Curve 2D and a computer program that was developed with Microsoft Excel to derive values for the variable parameters. The best fit for the data was a Langmuir model, which was used to plot equilibrium isotherms from triplicate analysis. The isotherm equation was entered as user-defined functions.

Estimates for the Q_{max} and K_d were taken from the double-logarithmic plot of the isotherm. The plot displays a break in the curve. The value on the x axis where the curve breaks is an estimate of K_d^{-1}. The value on the y axis where the curve breaks is an estimate of Q_{max} (Grant and Phillips 1998; Abdellaoui et al. 2019). The Q_{max} was taken from the fit of the Langmuir model to the adsorption data. Equations for the calculation of isothermal data are shown in Table 2.

Hydra Bioassay

Hydra vulgaris were obtained from Environment Canada (Montreal, Qc) and maintained at 18°C. The hydra classification method (Wilby et al. 1990) was used with modification to rate morphology of the adult hydra as an indicator of solution toxicity. In this assay, the scoring of hydra morphology is objective and repeatable as indicated in our previous literature. The assay included monitoring times at shorter intervals during the first two days (0, 4, 20, and 28 hr) and 24 hr intervals for the last three days (44, 68, and 92 hr). Solutions were not changed during testing. The hydra morphological response was scored and recorded after exposure to AfB_1, with and without, sorbent treatment. Mature and non-budding hydra in similar sizes were chosen for testing in order to minimize differences between samples. Controls for this experiment included hydra media consisting of 18.2 MΩ water, 4 mg L^{-1} ethylenediaminetetraacetic acid (EDTA), 115 mg L^{-1} N-tris[Hydroxymethyl]methyl-2-aminoethanesulfonic acid (TES), and 147 mg L^{-1} calcium dichloride ($CaCl_2$) adjusted to pH 6.9–7.0. Sorbent inclusion percentage was chosen based on previous studies (Phillips et al. 2008). Toxin treatment groups included 20 mg kg^{-1} AfB_1 in hydra media based on the minimum effective dose (MED) that caused 100% mortality in 92 hr. All test solutions were prepared by shaking at 1000 rpm for 2 hr and centrifugation at 2000 g for 20 min prior to toxin exposure of hydra in Pyrex dishes (Brown et al 2014). For each sample, three hydra were included into 4 mL of test media and kept at 18°C. The score or average toxicity rating was determined by calculating the average score for morphological changes for a certain group at a specific time point.

Molecular Models

The molecular model for bentonite was drawn in ISIS Draw 2.0 (MDL Information Systems, Inc., Hayward, California) and then imported into HyperChem 8.0. The aflatoxin structure was energy-minimized using the semiempirical quantum mechanical AM1 method. The model was constructed using the unit cell coordinates of muscovite (Richardson and Richardson 1982). These coordinates were then converted to orthogonal coordinates in an Excel spreadsheet that was constructed from a public domain C program. The unit cells were replicated in three-dimensional space by applying the symmetry operations for a C2/c space group (Donnay 1952). The d_{001} spacing of the model was then set to the corresponding dimensions of the bentonite (18 Å) based on the report of Greenland and Quirk (1960). The model was constructed in a 56 Å water box and aflatoxin was added to the interlayer and on the external basal surface (Slade et al. 1978), to illustrate proposed sites of aflatoxin sorption, based on isothermal data.

Statistical Analysis

A two way t-test was used to calculate statistical significance. Each experiment was independently triplicated to derive an average and standard deviation. In the t-test, the average COLE ratio from COLE experiments, Q_{max} from equilibrium isothermal analyses and toxicity scores from the hydra assay were included to calculate D = control-test groups and D^2. Then the t-value was calculated using the following equation (N = 3):

$$t = \frac{\frac{\sum D}{N}}{\sqrt{\frac{\sum D2 - \frac{(\sum D)2}{N}}{(N-1)N}}}$$

The t-value and degrees of freedom were compared in a p-value table to determine the statistical significance. Results were considered significant at $p \leq 0.05$.

Results

The COLE (Coefficient of Linear Expansibility) ratio indicates the expansibility of sorbents in water. COLE is equal to the expansion volume of clay divided by the original volume of clay. The higher the ratio, the more expansion and hydration of the sample. The accuracy of this method was confirmed by the COLE values for CB and SB clays, which showed limited swelling for CB compared to both SB clays (Figure 1). The COLE ratio for the test bentonite clay (SB-E) was equal to 5.85, indicating sodium predominance in its interlamellar region and the ability to swell upon hydration.

The isotherm in Figure 2A shows AfB_1 sorption at pH 6.5 onto the surface of SB-E compared to standard samples of CB and SB clays. For all isotherms, the r^2 values (or coefficients of determination) were above 0.8, indicating that the raw data strongly fit the Langmuir model and that AfB_1 was bound tightly onto the clay surfaces and did not dissociate easily. Sample SB-E showed the highest Q_{max} for AfB_1 with 0.42 moles of toxin bound per kg of clay. The K_d values (or binding affinities) for all sorbents were similar. In Figure 2B, isothermal plots at pH 2 indicated that the sorption of AfB_1 onto the surfaces of SB-E was significantly increased (Q_{max} equal to 0.6 mol/kg) compared to the plots at pH 6.5. To calculate the binding enthalpy of sample SB-E for AfB_1, isotherms were run at 2 different temperatures, i.e., 26°C (T_1) and 37°C (T_2). Calculated enthalpies (ΔH) for sample SB-E were equal to −61.7 kJ mol^{-1} at pH 6.5 and −46.6 kJ mol^{-1} at pH 2, which were similar to the standard CB (−89.2 kJ mol^{-1} and −36.8 kJ mol^{-1}, respectively) (Figure 3). After the interlayers of SB-E were heat-collapsed, the AfB_1 sorption was dramatically decreased (Figure 4). A summary of sorption parameters for AfB_1 onto active surfaces of standard CB and SB, and SB-E is shown in Table 3.

In order to establish the amount of sorbent needed to mitigate different levels of aflatoxin in a contaminated diet, % toxin sorption can be plotted against sorbent inclusion level ([S]) to derive the dose of sorbent needed to achieve the regulatory level. We exposed AfB_1 at twice the 20 ng g^{-1} threshold level (or 40 ng g^{-1}) to an increasing dose of sorbent ranging from 0.0001% to 0.002%. Based on our dosimetry results (Figure 5), to reduce 50% aflatoxin exposure and thus achieve below the action level, the predicted sorbent inclusion rate ([S]) for SB-E would be equal to 0.01%, which was 8 times less than the predicted dose for standard CB (i.e. 0.08%).

The minimum effective dose (MED) for AfB_1 in the hydra bioassay has been established earlier as 20 mg kg^{-1}, which results in 100% hydra mortality in 92 hr (Wang et al. 2019). All

sorbents at the inclusion rate at 0.5% showed no adverse effects in hydra (Figure 6A). When SB-E was included at a very low clay inclusion rate of 0.02% in the presence of 20 mg kg^{-1} AfB_1, complete protection of hydra against AfB_1 was achieved compared to the hydra media control (Figure 6B). Based on the evidence from isothermal and hydra studies, a molecular model representing aflatoxin binding interactions on active surfaces within the interlamellar region of SB-E is shown in Figure 7. The molecular models of CB and SB have been previously published along with XRD analysis (Marroquin-Cardona et al. 2011a, 2011b; Zychowski 2014). There are no major differences in the unit cell formulas for SB and SB-E.

Discussion

Based on our previous *in vitro* work and extensive animal interventions and human clinical trials, CB clay was an effective aflatoxin enterosorbent and was safe for consumption by humans and animals (Phillips et al. 2019). The interlayers of SB are more accessible than CB, but may be less preferential than CB. The high expansibility and dispersion in water for SB was confirmed by its COLE ratio equal to 8.33, whereas CB was shown to have limited swelling as indicated by its COLE ratio of 2.02 (Figure 1). The stronger swelling tendency of SB is related to the increased hydration energy of sodium ions versus calcium ions. This facilitates the hydration and desorption of sodium from interlamellar regions following the addition of water and swelling. Sample SB-E showed a high COLE value, indicating a predominance of sodium in the structure. SB-E also showed the ability to quickly flocculate and precipitate after 24 hr of equilibrium. Thus, we suspect that the unusual combination of a high COLE value (like SB) and a high flocculation ability (like CB) could be associated with the sodium adsorption ratio and contribute to the higher aflatoxin sorption capacity of SB-E. Further work (*in vitro* and *in vivo*) will elucidate this mechanism and investigate the enhanced ability of SB-E to protect against aflatoxicosis in animals and humans.

CB and SB are commonly used as general sorbents for toxin binding (Abdellaoui et al. 2019). To investigate the binding effectiveness for AfB_1, equilibrium isotherms were generated by Table-Curve 2D and a computer program was developed in our laboratory using Microsoft Excel. This program was used to derive affinities (K_d), capacities (Q_{max}) and the enthalpy of sorption (ΔH) for toxin-surface interactions. Based on r^2 values ($r^2 > 0.8$) and randomness of the residuals, the best fit for the data was a Langmuir model, which was used to plot equilibrium isotherms from triplicate analyses. Each point represents the values calculated for AfB_1 bound to clay (mol/kg) and AfB_1 left in solution (mol/L) for the corresponding dilutions. Although the expansibility of SB standard in water was larger than CB standard, its binding capacity was typically lower, as shown in Figure 2A. When isotherms were run at pH 6.5, simulating the pH of the intestine, SB-E showed the highest Q_{max}, which was equal to 0.42 mol/kg for AfB_1 sorption. This value was higher than that of CB (i.e. 0.35 mol/kg). Further work is ongoing to delineate reasons for a uniformly higher binding capacity of SB-E vs CB. At pH 2, SB-E showed increased Q_{max} and decreased K_d values, compared to pH 6.5 (Figure 2B). This resulted in a significantly increased Q_{max} for SB-E vs CB. Since the pH_{PZC} (pH for zero point of charge) of bentonite is 2–3, a possible mechanism for this effect in SB-E may involve acidic solution providing protons that can neutralize the overall negative charge at active surfaces in the interlamellar region and

decrease binding affinity leading to increased Q_{max}. SB-E was a very efficient clay binder for AfB_1 at pH 2, and this pH will be the first encountered by clay and the toxin in the diet of humans and monogastric animals.

As part of this study, it was important to gain insight into AfB_1 binding mechanisms and the thermodynamics of toxin/surface interactions. The enthalpy (heat) of sorption (ΔH) can be calculated from K_d values of isotherms run at different temperatures. It is directly relevant to the tightness of toxin/clay interactions and can help with the derivation of mechanistic information (Fischer and Peters 1970; Stumm et al. 1992). In particular, the sorption of compounds to a surface can be categorized as either physisorption or chemisorption on the basis of ΔH (Gatta 1985). Physisorption involves weak associations, which include Van der Waals attraction, dipole−dipole interactions, induced dipole interactions, and hydrogen bonding. Chemisorption implies a chemical reaction or sharing of electrons between the adsorbent and the adsorbate. Physisorption is described as having an enthalpy of < 20 kJ mol $^{-1}$, while chemisorption is generally > 20 kJ mol^{-1} (Gu et al. 1994). Sorption enthalpy (ΔH) for clay interactions with AfB_1 were calculated by the Van't Hoff equation from isotherms at 2 different temperatures, i.e., 26°C (T_1) and 37°C (T_2). Derived ΔH values for sample SB-E (−61.7 kJ mol^{-1} and −46.6 kJ mol^{-1}, at pH 6.5 and 2, respectively) were similar to CB (−89.2 kJ mol^{-1} and −36.8 kJ mol^{-1}, respectively) (Figure 3). These high enthalpy absolute values indicate that AfB_1 is chemisorbed tightly to the clay surfaces and is consistent with a Langmuir model for the isothermal interaction. Following heating, the interlayers of CB and sample SB-E were dehydroxylated and collapsed. Figure 4 showed that binding capacities of collapsed CB and collapsed SB-E were significantly reduced. This dramatic decrease of AfB_1 suggests (indirectly) that a large amount of the AfB_1 binds within the negatively charged interlayer of these clays and only minor amounts bind on the edges and basal surfaces. A summary of sorption parameters for AfB_1 onto surfaces of CB, SB, and SB-E is shown in Table 3.

Besides isotherms, enhanced binding efficacy of SB-E was also shown in our dosimetry study that delineated the amount of clays required to maintain a regulatory threshold concentration of AfB_1 (20 ng g^{-1}). Based on our results (Figure 5), for 40 ng g^{-1}, the predicted concentration of sorbent ([S]) for CB and was equal to 0.08% inclusion in the diet, which is equivalent to 2.4 g clay/day based on a 3 kg daily intake in the U.S. for humans. This level is in agreement with our earlier mass balance study with CB in animals, where 0.1% inclusion in the diet significantly decreased exposures from 80 and 40 ng g^{-1} of ^{14}C-AfB_1 labeled aflatoxin. For SB-E, [S] was equal to 0.01% or 0.3 g clay/kg of diet based on a daily intake of 3 kg for U.S. adults. This level of SB-E clay (if approved for human consumption) could be easily delivered as three 0.2 g doses before each meal.

The protective roles of CB, SB, and SB-E were confirmed *in vivo* using the adult hydra assay. As indicated in Figure 6A, the clays were not toxic to the hydra and were comparable to the hydra media control (morphological score of 10). In further studies, 20 mg kg^{-1} AfB_1 resulted in 100% mortality of hydra within 92 hr. Importantly, SB-E at a 0.02% inclusion in hydra media showed complete (100%) protection against 20 mg kg^{-1} AfB_1 (Figure 6B). Because this work was focused on characterizing a high capacity binder for aflatoxin, we

included levels of clays (0.02%) in the hydra bioassay that were less than the common inclusion level in animal feed (0.2%). Our findings *in vivo* are consistent with our *in vitro* isothermal results.

Based on *in vitro* and *in vivo* results, a suggested model for AfB_1 sorption to SB-E surfaces is shown in Figure 6. Sample SB-E showed the highest binding capacity for aflatoxin at pH 6.5 and pH 2 with high enthalpy (ΔH) and was very effective as a binder for high doses of aflatoxins. Heat-collapsed CB and SB-E indicated that the major binding sites for AfB_1 were on surfaces within the interlayer (Figure 7). The hydra bioassay also confirmed the safety of SB-E and its ability to protect against aflatoxin at low rates of clay inclusion. SB deposits are widespread, and this material, which is highly effective for aflatoxin binding, should be applicable for use in animal feed. SB binders (like SB-E) could be delivered through capsules, nutritional supplements, snacks, flavored liquids and complete feeds during emergencies and outbreaks of acute aflatoxicosis.

Acknowledgments

This work was supported by the NIEHS (Superfund hazardous Substance Research and Training Program) under Grant number P42 ES0277704; and USDA under Grant number Hatch 6215.

References

Abdellaoui Y, Olguinm MT, Abatal M, Ali B, Mendez SED, Santiago AA. 2019 Comparison of the divalent heavy metals (Pb, Cu and Cd) adsorption behavior by montmorillonite-KSF and their calcium- and sodium-forms. Superlattice Microst. 127:165–175.

Allcroft R, Carnaghan RBA. 1963 Groundnut Toxicity: An examination for toxins in human food products from animals fed toxic groundnut meal. Vet Rec. 75:259–263.

Brown KA, Mays T, Romoser A, Marroquin-Cardona A, Mitchell NJ, Elmore SE, Phillips TD. 2014 Modified hydra bioassay to evaluate the toxicity of multiple mycotoxins and predict the detoxification efficacy of a clay-based sorbent. JAT. 34:40–48. [PubMed: 23047854]

[CAST] Council for Agricultural Science and Technology. 1989 In mycotoxins: Economic and health risks In: Niyo K, editor. Task Force Report. Ames (USA): CAST; p. 1–91.

Donnay JD. 1952 International tables for X-ray crystallography. Birmingham (USA): Kynoch Press; p. 3.

[EC] European Commission. 2005 Soil atlas of europe, european soil bureau network. Luxembourg: Office for Official Publications of the European Communities; p. 128.

Egner PA, Wang JB, Zhu YR, Zhang BC, Wu Y, Zhang QN, Qian GS, Kuang SY, Gange SJJacobson LP. 2001 Chlorophyllin intervention reduces aflatoxin–DNA adducts in individuals at high risk for liver cancer. Proc Natl Acad Sci USA, 98(25): 14601–14606. [PubMed: 11724948]

Fallingborg J 1999 Intraluminal pH of the human gastrointestinal tract. Dan. Med. Bull. 46(3):183–196. [PubMed: 10421978]

Fischer RB, Peters DG. 1970 Chemical equilibrium. Philadelphia (USA): W. B. Saudners; p. 1.

Gatta GD. 1985 Direct determination of adsorption heats. Thermochim. Acta. 96:349–363.

Grant PG, Phillips TD. 1998 Isothermal adsorption of aflatoxin B(1) on HSCAS clay. J Agric Food Chem. 46:599–605. [PubMed: 10554284]

Greenland DJ, Quirk JP. 1960 Adsorption of 1-n-alkyl pyridinium bromides by montmorillonite. Clays Clay Miner. 9:484–499.

Gu B, Schmitt J, Chen Z, Liang L, McCarthy JF. 1994 Adsorption and desorption of natural organic matter on iron oxide: mechanisms and models. Environ Sci Technol. 28:38–46. [PubMed: 22175831]

Kensler TW, Chen JG, Egner PA, Fahey JW, Jacobson LP, Stephenson KK, Ye L, Coady JL, Wang JB, Wu Y. 2005 Effects of glucosinolate-rich broccoli sprouts on urinary levels of aflatoxin–DNA adducts and phenanthrene tetraols in a randomized clinical trial in He Zuo township, Qidong, People's Republic of China. Cancer Epidemiol Biomarkers Prev, 14(11 Pt 1): 2605–2613. [PubMed: 16284385]

Khlangwiset R, Wu F. 2010 Costs and efficacy of public health interventions to reduce aflatoxin-induced human disease. Food Addit Contam Part A, 27(7): 998–1014.

Marroquin-Cardona A, Deng Y, Garcia-Mazcorro J, Johnson NM, Mitchell N, Tang L, Robinson A, Taylor J, Wang JS, Phillips TD. 2011a Characterization and safety of uniform particle size NovaSil clay as a potential aflatoxin enterosorbent. Appl Clay Sci. 54(3–4):248–257. [PubMed: 22249378]

Marroquin-Cardona AG. 2011b Characterization and safety of clays as potential dietary supplement to prevent aflatoxicosis [dissertation]. College Station (TX): Texas A&M University.

Murugesan GR, Ledoux DR, Naehrer K, Berthiller F, Applegate TJ, Grenier B, Phillips TD, Schatzmayr G. 2015 Prevalence and effects of mycotoxins on poultry health and performance, and recent development in mycotoxin counteracting strategies. Poult Sci. 94:1298–1315. [PubMed: 25840963]

Phillips TD, Afriyie-Gyawu E, Williams J, Huebner H, Ankrah NA, Ofori-Adjei D, Jolly P, Johnson N, Taylor J, Marroquin-Cardona A, Xu L, Tang L, Wang JS. 2008 Reducing human exposure to aflatoxin through the use of clay: a review. Food Addit Contam Part A. 25(2):134–145.

Phillips TD, Sarr AB, Grant PG. 1995 Selective chemisorption and detoxification of aflatoxins by phyllosilicate clay. J Nat Toxins. 3:204–213; discussion 221.

Phillips TD, Wang M, Elmore SE, Hearon S, Wang JS. 2019 NovaSil clay for the protection of humans and animals from aflatoxins and other contaminants. Clays Clay Miner. 67(1):99–110.

Richardson SM, Richardson JM. 1982 Crystal structure of a pink muscovite from Archer's post, Kenya: implications for reverse plechorism in dioctahedral micas. Am Miner. 67:69–75.

Slade PG, Raupach M, Emerson WW. 1978 The Ordering of Cetylpyridinium Bromide on Vermiculite. Clays Clay Miner. 26:125–134.

Stumm W, Sigg L, Sulzberger B. 1992 Chemistry of the solid-water interface. New York (USA): Wiley; pp. 1.

Tang L, Tang M, Xu L, Luo H, Huang T, Yu J, Zhang L, Gao W, Cox SB, Wang JS. 2008 Modulation of aflatoxin biomarkers in human blood and urine by green tea polyphenols intervention. Carcinogenesis, 29(2): 411–417. [PubMed: 18192689]

Thuresson A, Jansson M, Plivelic TS, Skepö M. 2017 Temperature response of charged colloidal particles by mixing counterions utilizing Ca2+/Na+ montmorillonite as model system. J Phys Chem C. 121(14):7951–7958.

[USDA] United States Department of Agriculture. 1978 Engineering Classification of Earth Materials. In National Engineering Handbook, Part 631.

Wang JS, Shen X, He X, Zhu YR, Zhang BC, Wang JB, Qian GS, Kuang SY, Zarba AEgner PA. 1999 Protective alterations in phase 1 and 2 metabolism of aflatoxin B1 by oltipraz in residents of Qidong, People's Republic of China. J Natl Cancer Inst, 91: 347–354. [PubMed: 10050868]

Wang M, Hearon S, Phillips TD. 2019 Development of enterosorbents that can be added to food and water to reduce toxin exposures during disasters. J Environ Sci Heal B. 54(6):514–524.

Wang M, Hearon SE, Johnson NM, Phillips TD. 2019 Development of broad-acting clays for the tight adsorption of benzo[a]pyrene and aldicarb. Appl Clay Sci. 168:196–202. [PubMed: 31435120]

Wang M, Maki CR, Deng Y, Tian Y, Phillips TD. 2017 Development of high capacity enterosorbents for aflatoxin B1 and other hazardous chemicals. Chem Res Toxicol. 30(9):1694–1701. [PubMed: 28768106]

Wang P, Afriyie-Gyawu E, Tang Y, Johnson NM, Xu L, Tang L, Huebner HJ, Ankrah NA, Ofori-Adjei DEllis W. 2008 NovaSil clay intervention in Ghanaians at high risk for aflatoxicosis: II. Reduction in biomarkers of aflatoxin exposure in blood and urine. Food Addit Contam, 25(5): 622–634.

Wilby OK, Tesh JM, Shore PR. 1990 Application of the hydra regeneration assay: Assessment of the potential teratogenic activity of engine exhaust emissions. Toxicology in vitro. 4:612–613. [PubMed: 20702240]

Zychowski KE. 2014 Calcium montmorillonite for the mitigation of aflatoxicosis and gastrointestinal inflammation [Dissertation]. College Station (TX): Texas A&M University.

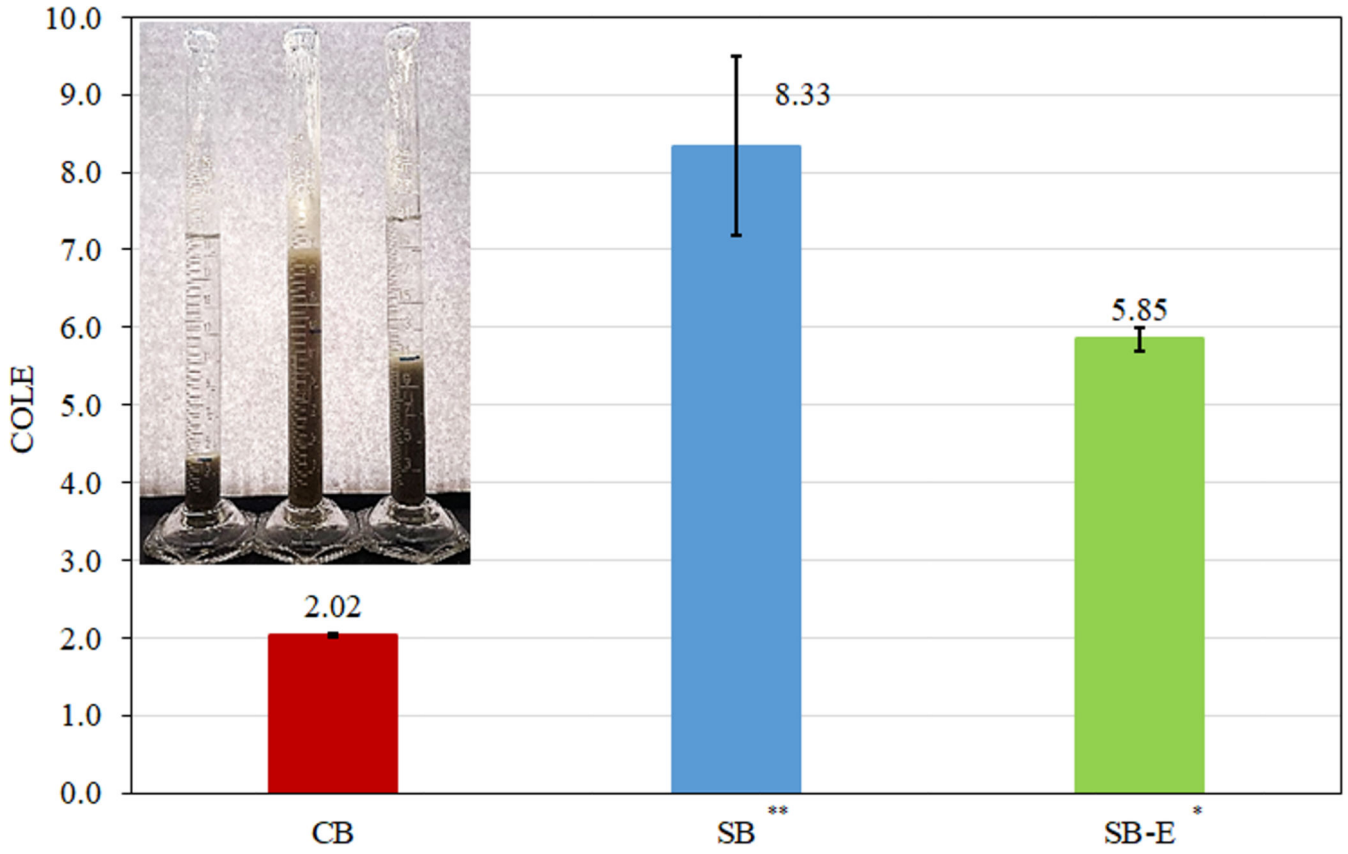

Figure 1.

Coefficient of linear expansibility for sorbents in water. The COLE value for CB confirmed its limited expansibility, whereas COLE values for SB and SB-E were significantly increased.

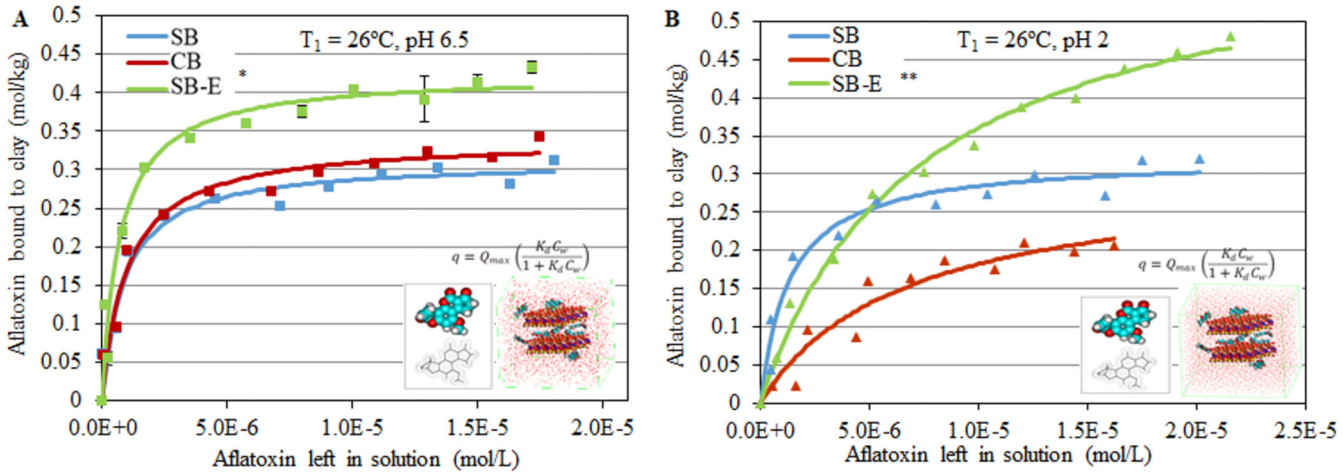

Figure 2.

Langmuir adsorption isotherm - plots of AfB_1 on SB, CB and SB-E showing the observed and predicted Q_{max} values at 26°C (T_1), pH 6.5 (A) and pH 2 (B) (* $p \leq 0.05$, ** $p \leq 0.01$).

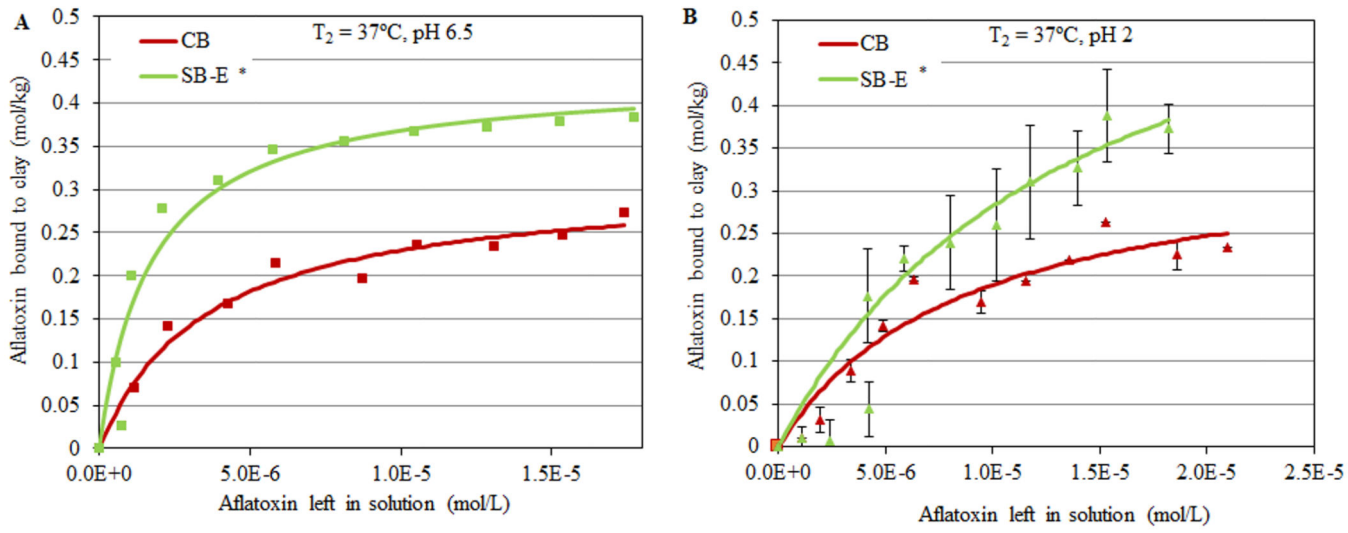

Figure 3.

Langmuir adsorption isotherm - plots of AfB_1 on CB and SB-E showing the observed and predicted Q_{max} values at 37°C (T_2), pH 6.5 (A) and pH 2 (B) (* $p \leq 0.05$).

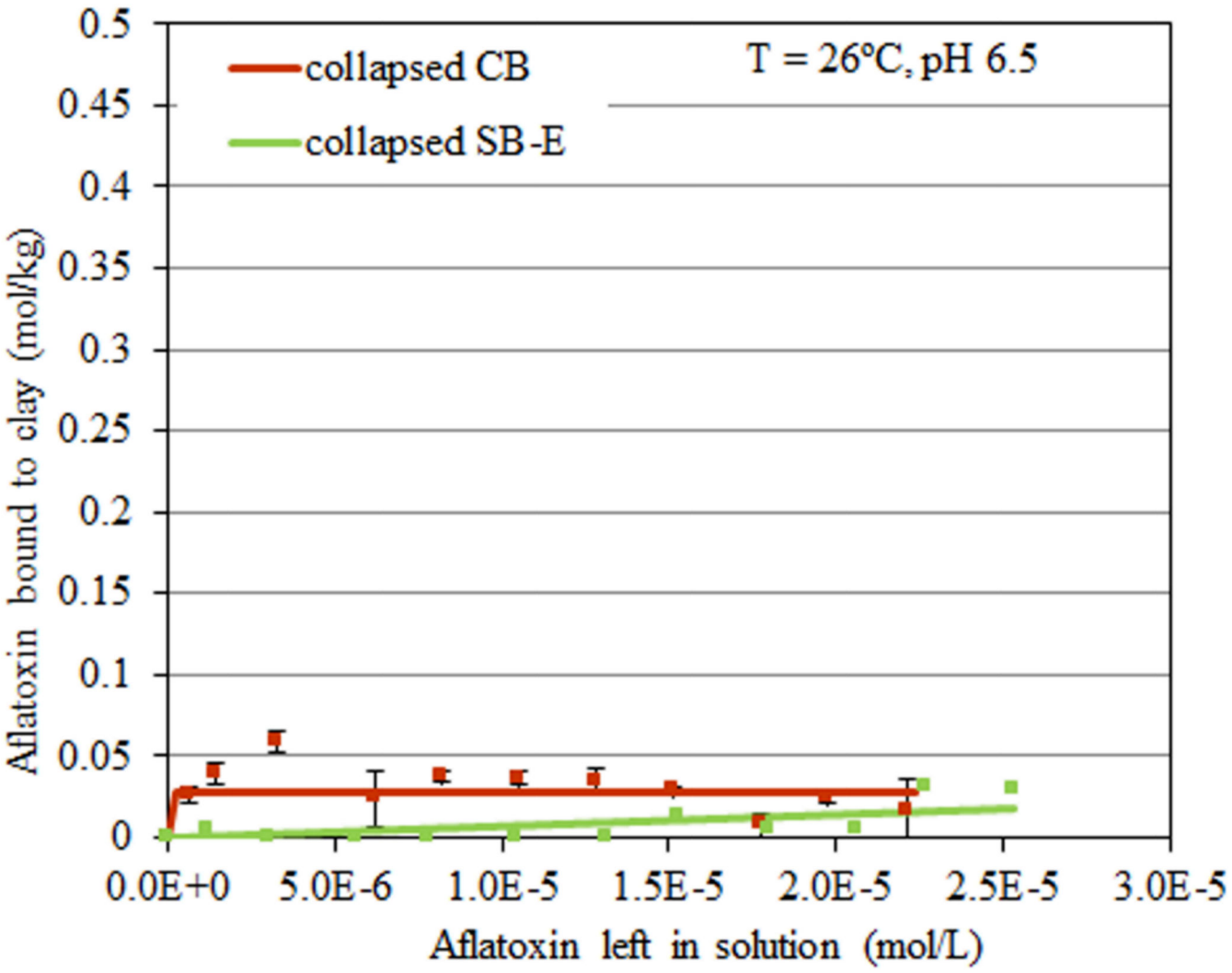

Figure 4.
Langmuir adsorption isotherm - plots of AfB_1 on collapsed CB and collapsed SB-E at 26°C and pH 6.5.

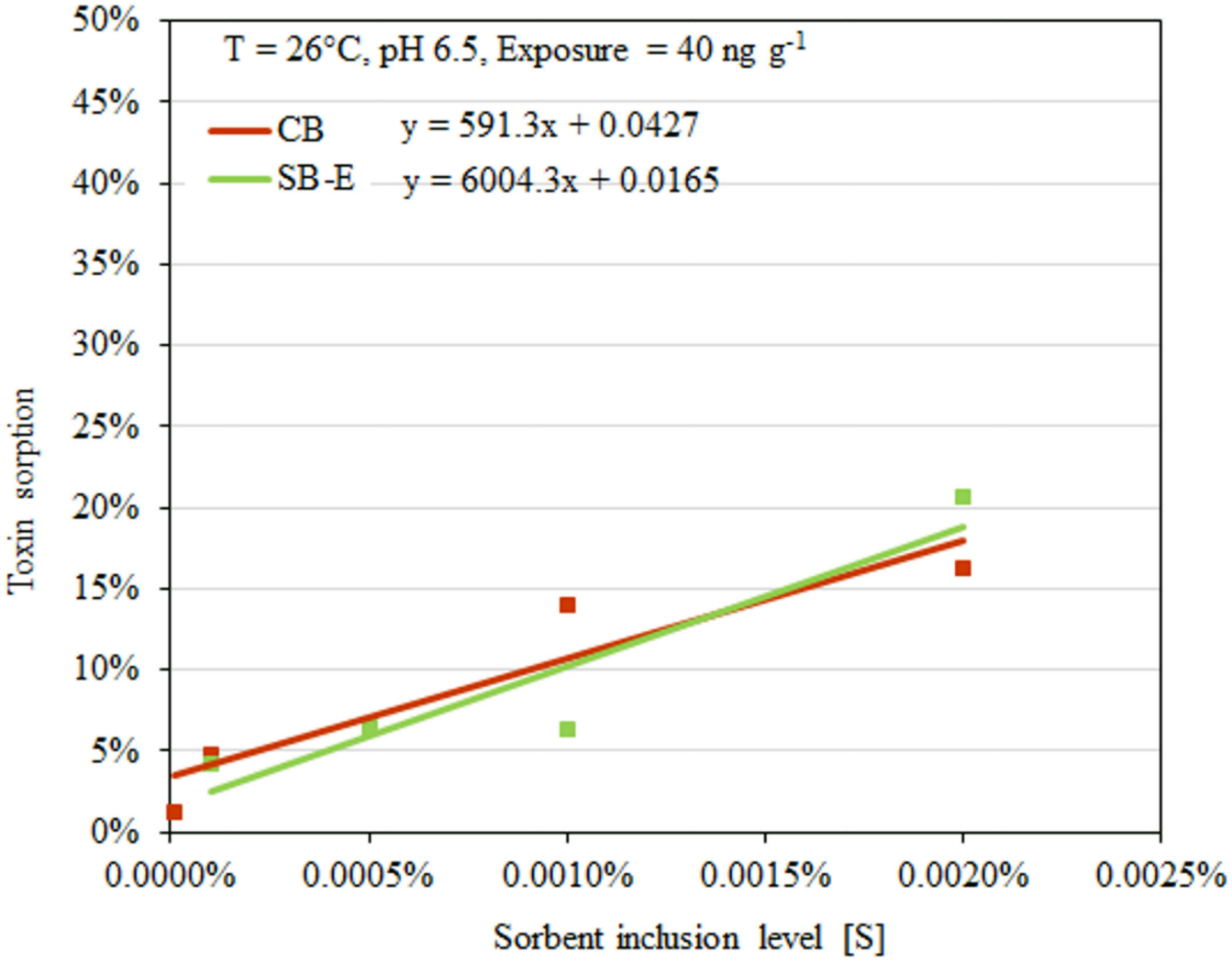

Figure 5.
Extrapolation of sorbent dosimetry for aflatoxin exposure at 40 ng g^{-1}.

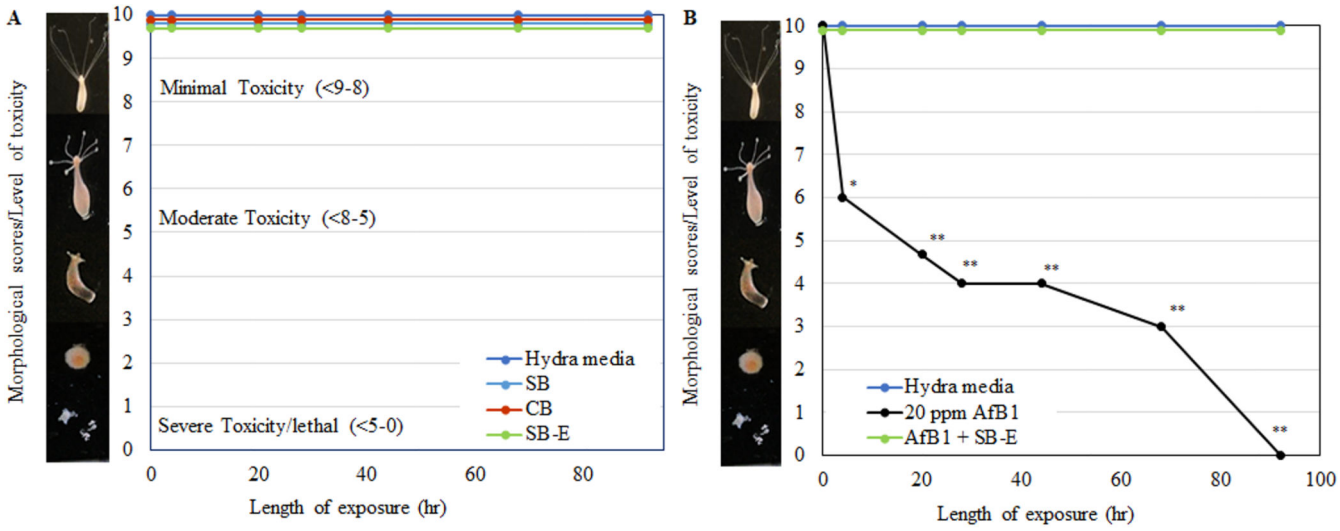

Figure 6.

Hydra bioassay of bentonite samples at a 0.5% inclusion rate (A), and protection at a 0.02% inclusion rate of SB-E are shown in the presence of 20 mg kg^{-1} AfB_1 (B). Hydra media and toxin controls are included for comparison. No toxicity was shown by the hydra media and all clay treatment groups (* $p \leq 0.05$, ** $p \leq 0.01$).

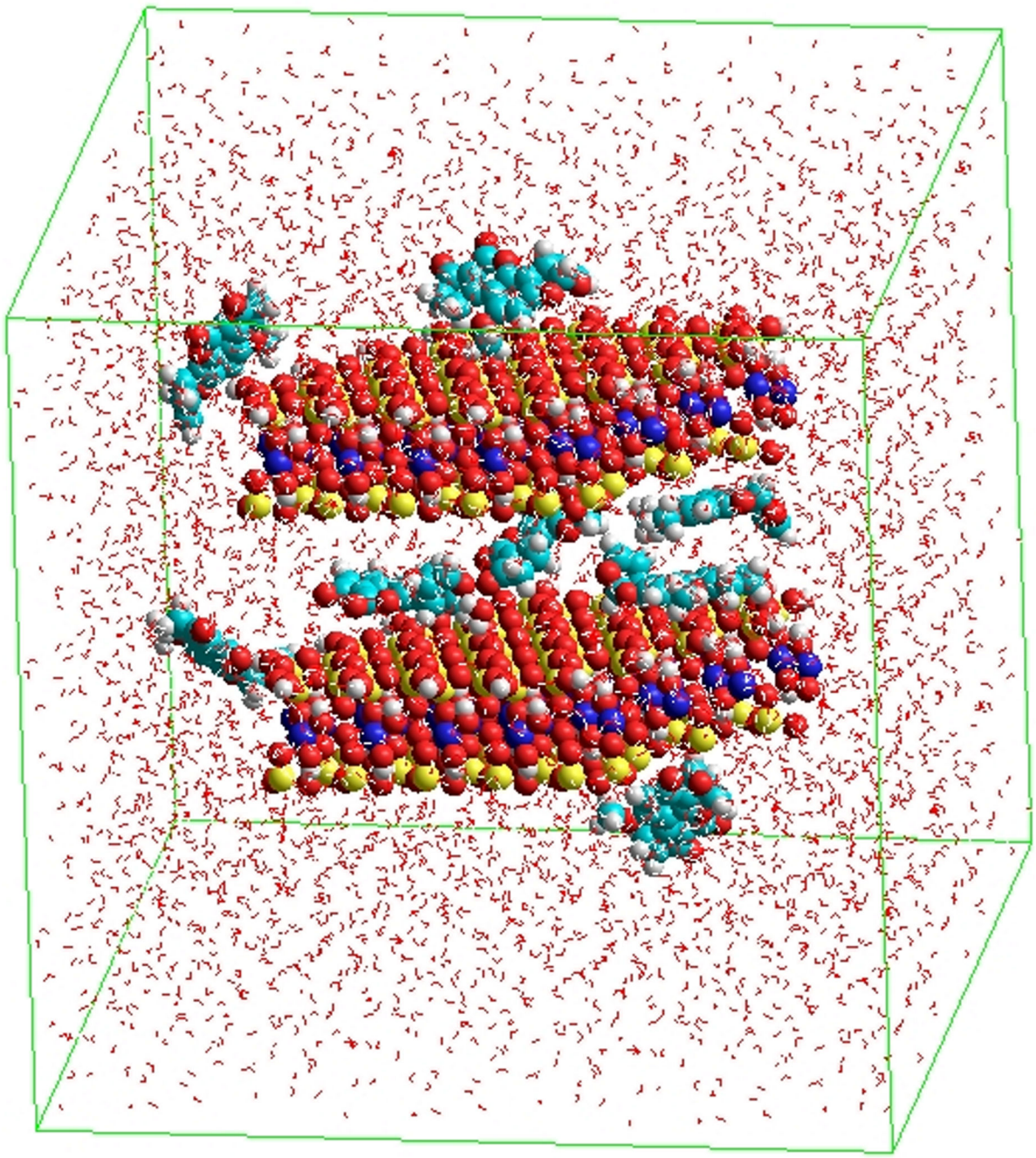

Figure 7.

Energy minimized molecular model of SB-E and aflatoxin B_1 in a water box (oxygen = red; silicon = yellow; aluminum = blue; carbon = cyan).

Table 1.

Important physico-chemical properties of CB, SB and SB-E

	CB	SB	SB-E
Appearance	Off-white to grayish-green powder	Off-white powder	Blue, gray powder
Bulk density (loose)	640.74 kg/m^3	593 kg/m^3	849 kg/m^3
Moisture	9%	8%	9–12%
Screen analysis	5% +100 mesh	80% −200 mesh	0-5% + 60 mesh
	18% +200 mesh	80% −200 mesh	15-25% +100 mesh
	60% −325 mesh		70-80% −200 mesh
Chemical analysis by X-ray fractionation (XRF) spectroscopy (weight %)	%CaO 3.2-4.8	%CaO 1.68	%CaO 2.64
	%MgO 4.0-5.4	%MgO 0.05	%MgO 1.83
	%Fe_2O_3 5.4-6.5	%Fe_2O_3 3.35	%Fe_2O_3 3.72
	%K_2O 0.50-0.90	%K_2O 0.53	%K_2O 0.6
	%Na_2O 0.10-0.30	%Na_2O 1.53	%Na_2O 2.51
	%MnO 0.01-0.03	%MnO 0.006	%MnO 0.08
	%Al_2O_3 14.8-18.2	%Al_2O_3 19.6	%Al_2O_3 17.6
	%SiO_2 62.4-73.5	%SiO_2 62.9	%SiO_2 59.9

(Data collected from product information sheets and clays.org)

Table 2.

Equations for the calculation of isothermal data

Beer's law	Absorbance = Ɛ L c $\mathcal{E}$ is the molar extinction coefficient (Ɛ for AfB_1 = 21,865 $cm^{-1}mol^{-1}$), L is the path length of the cell holder = 1 cm.
Langmuir model	$q = Q_{\max}(\frac{K_d C_w}{1 + K_d C_w})$ q = AfB_1 sorbed (mol/kg), Q_{max} = maximum capacity (mol/kg), K_d = distribution constant, C_w = equilibrium concentration of AfB_1.
K_d	$K_d = \frac{q}{(Q_{\max} - q)C_w}$

Table 3.

Summary table of sorption parameters for CB, SB and SB-E.

Sorbents	pH 6.5, T_1	pH 2, T_1	pH 6.5, T_2	pH 2, T_2	Collapsed
SB	Q_{max} = 0.31	Q_{max} = 0.32	N/A	N/A	N/A
	K_d = 1.2E6	K_d = 7.5E5			
CB	Q_{max} = 0.35	Q_{max} = 0.3	Q_{max} = 0.32	Q_{max} = 0.35	Q_{max} = 0.03
	K_d = 9.0E5	K_d = 1.5E5	K_d = 2.8E5	K_d = 1.2E5	K_d = 4.2E19
SB-E	Q_{max} = 0.42	Q_{max} = 0.62	Q_{max} = 0.43	Q_{max} = 0.68	K_d = 1.5E2
	K_d = 1.4E6	K_d = 1.4E5	K_d = 5.8E5	K_d = 7.2E4	

(SB, sodium montmorillonite; CB, calcium montmorillonite; SB-E, sample E; T_1 = 26°C; T_2 = 37°C; Q_{max} = maximum capacity; K_d = affinity constant; N/A, not applicable)